

Narrow linewidth single laser source system for onboard atom interferometry

F. Theron,^{1,*} O. Carraz,² G. Renon,¹ Y. Bidel,¹ N. Zahzam,¹ M. Cadoret,³ and A. Bresson¹

¹*ONERA - The French Aerospace Lab, BP 80100, 91123 Palaiseau Cedex, France*

²*European Spatial Agency - ESTEC Future Missions Division (EOP-SF) P.O. Box 299, 2200 AG Noordwijk, The Netherlands*

³*Laboratoire Commun de Métrologie CNAM, 61 rue du Landy, 93210 La Plaine Saint Denis, France*

**Corresponding author: fabien.theron@onera.fr*

Compiled August 30, 2019

We present an original compact and robust laser system for atom interferometry based on a frequency-doubled telecom laser. Thanks to an original stabilization architecture on a saturated absorption, we obtain a frequency agile laser system allowing fast tuning of the laser frequency over 1 GHz in few ms using only a single laser source. The different laser frequencies used for atom interferometry are created by changing dynamically the frequency of the laser and by creating sidebands using a phase modulator. We take advantage of the maturity of fiber telecom technology to reduce the number of free-space optical components, which are intrinsically less stable, and to make the setup compact, much less sensitive to vibrations and thermal fluctuations. This source provides spectral linewidth below 2.5 kHz required for precision atom interferometry, and particularly for an high performance atomic inertial sensor. © 2019 Optical Society of America

OCIS codes: 020.1335, 020.3320, 120.3180.

Atom interferometers have demonstrated excellent performances for precision acceleration and rotation measurements [1]. Many applications of these sensors, as tests of fundamental physics in space [2] or gravimetry [3], need the setup to be compact, transportable and robust in order to operate in relevant environment. Many researches have been made the last few years to develop transportable laser systems [4–7] and in particular laser systems as compact and immune to perturbations as possible.

Atom interferometers usually operate with alkali atoms by driving transitions in the near-IR spectrum (852 nm for Cs, 780 nm for Rb, and 767 nm for K). Light pulse atom interferometer sequence consists usually in three stages. First, a gas of atoms is cooled, trapped and prepared in a non sensitive magnetic state. Then, these cold atoms are illuminated by a serie of three light pulses driving stimulated Raman transitions performing a Mach-Zehnder type atom interferometer [8]. Finally, the phase shift of the interferometer is deduced from fluorescence measurements. In these experiments, we need several stable laser frequencies relative to atomic transition of alkali used : one cooling and trapping frequency, one repumping frequency, two Raman frequencies and one detection frequency. The spectral linewidth of the laser need to be smaller than the linewidth of the atomic transition for the cooling stage (6 MHz for Rb). To realize stimulated Raman transitions, we need an even narrower linewidth laser because the frequency noise of the laser induces a noise on the atom interferometer measurement [9]. This aspect is very important for gravity gradiometers for which the sensitivity is not limited by vibrations.

Different technologies of laser sources are available

for addressing alkali atoms. First, one can use laser sources emitting directly on the atomic transition of the atoms : Distributed FeedBack lasers (DFB), Distributed Bragg Reflector lasers (DBR) and Extended-Cavity Diode Lasers (ECDL) [10]. The disadvantage of these technologies is that one has to provide a lot of efforts to get robust systems, immune to mechanical misalignments caused by vibrations, for onboard applications. Another appropriate solution, for Rb and K, is to use frequency-doubled telecom lasers operating around 1.5 μm [11, 12]. This technique is based on the maturity of the fiber components in the telecom C-band to reduce the amount of free-space optics and to make the setup more compact and less sensitive to misalignments. Moreover, many types of narrow linewidth laser sources are commercially available such as DFB laser, DFB with whispering-gallery-mode resonator [13], integrated ECLD diodes [14] and Erbium Fiber DFB Laser (EFL). In this article, we will present results obtained with an EFL sources which has already been used for atom interferometry [4].

There are several architectures to obtain all the laser frequencies needed for an atom interferometer experiment. The most common one uses at least two lasers : a master laser and a slave laser [4–6]. The master laser has a fixed frequency and is locked on an atomic transition. The slave laser is locked relatively to the master laser thanks to a beat note. By changing the set point of the beat note lock, it is possible to change dynamically the frequency of the slave laser and to address all the functions needed for atom interferometry. For onboard applications where one needs compact and robust laser system, the use of two laser sources is not suitable. Indeed, by using only one laser source, the size of the laser

system is decreased, the risk of failure of the system due to laser source breakdown is reduced and the electrical consumption is lower.

In this article, we present a laser system for Rubidium atom interferometry using only one laser source based on a frequency doubled telecom fiber bench. A laser system, tunable in few ms, within a frequency range of typically 1 GHz, can generate cooling, detection and the first Raman frequencies. The repumping frequency and the second Raman frequency can be obtained by creating sidebands on the previous laser source. For our system, the laser source is a narrow linewidth EFL, which can be frequency tunable thanks to its piezoelectric actuator (PZT) (Fig. 1). In order to frequency stabilize the laser, one part of the laser output goes through a phase modulator (PM1) which generates side bands, then goes through a PPLN waveguide crystal which performs second harmonic frequency conversion and finally goes in a Rubidium saturated absorption set up [15] in which the first modulated order of the laser spectrum is locked to the cross over $F = 3 \rightarrow F' = 3$ c.o. 4 of the ^{85}Rb -D₂ line (Fig. 2). With a modulation at $\nu_1 = 1070$ MHz, the laser carrier (0 laser order) is in resonance with the detection transition $F = 2 \rightarrow F' = 3$ of the ^{87}Rb -D₂ line. By changing the frequency modulation ν_1 on the PM1, the first laser order stays locked on the atomic transition whereas only the frequency of the carrier is changed. In that case, the new carrier is detuned relative to the detection transition by $1070 \text{ MHz} - \nu_1$. In summary, the first sideband is locked on the deepest saturated absorption peak of the Rubidium 85, while the carrier is tuned on the Rubidium 87 transitions. With this technique, a frequency tuning range of at least 1 GHz at 780 nm can be obtained thus addressing all the functions needed for atom interferometry.

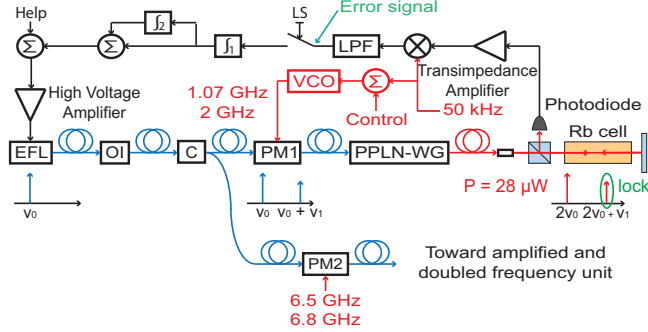


Fig. 1. Diagram of the laser system and the electronic lock : EFL, Erbium Fiber DFB Laser; OI, Optical Isolator; PM, Phase Modulator; C, fiber Coupler; PPLN-WG, Periodically Poled Lithium Niobate crystal - Wave Guide; VCO, Voltage Controlled Oscillator; LPF, Low Pass Filter; LS, Lock Switch (open during the frequency step); ν_0 , optical EFL frequency; ν_1 , frequency modulation of the PM1.

The frequency stabilization is achieved by modulating at 50 kHz the frequency ν_1 sent to the PM1, and

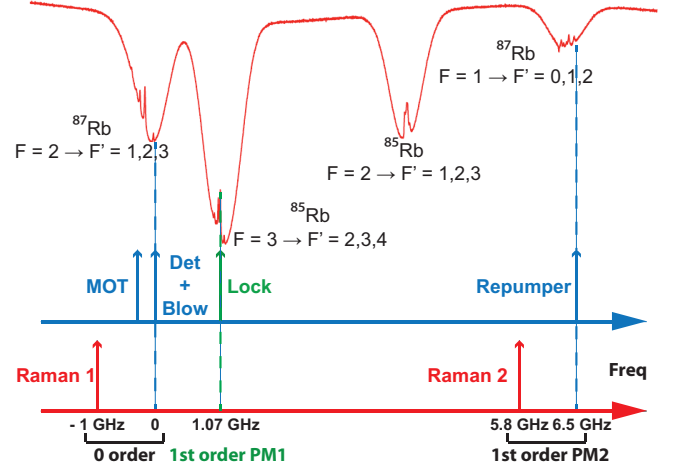


Fig. 2. Saturated absorption peaks of the D₂ Rubidium transition and laser frequencies generated for atom interferometry (laser frequencies for the cooling and detection stages in blue, and for the interferometric stage in red).

by collecting saturated absorption signal with a photodiode. The laser power used for this saturated absorption is equal to $28 \mu\text{W}$. Then this signal is amplified through a transimpedance amplifier, demodulated at 50 kHz and low pass filtered, hence providing at this point the dispersive error signal of the lock proportionnal to the frequency difference between the first order of the laser spectrum and the atomic frequency transition. Finally, it is integrated and amplified by a high voltage amplifier, and sent to the PZT of the EFL with a feedback bandwidth of 3 kHz (Fig. 1). We adjust the amplitude of the 50 kHz modulation in order to get the steepest slope. With this architecture, we get a capture range of 45 MHz on the error signal (Fig. 3). This finite range is due to the presence of the absorption peaks located before and after the peak where we are locked.

In order to improve the stability and to reduce the response time of the lock during frequency steps, a voltage signal ("Help" on Fig. 1) proportionnal to the frequency of the VCO is added to the corrected signal sent to the PZT. During the maximum frequency step of 1 GHz, the frequency deviation is too large compared to the lock range to allow the laser to stay locked. Thus, a lock switch (LS) is introduced just before the integrator to open the feedback loop during 1 ms after the frequency step. A second integrator stage is also added to reduce the stabilization time. After a frequency step of 1 GHz, the laser frequency is stabilized below 100 kHz after 3 ms (Fig. 3).

With this laser architecture, to get the second Raman frequency and the repumper required to realize the experiment (Fig. 2), we modulate the laser (detection or first Raman) at a frequency of 6.5 or 6.8 GHz with a fibered phase modulator at $1.5 \mu\text{m}$ (PM2 on Fig. 1) [16]. Finally, the laser is amplified in an Erbium Doped Fiber Amplifier (EDFA) and sent in a frequency doubling unit. The frequency doubling could be done thanks to PPLN

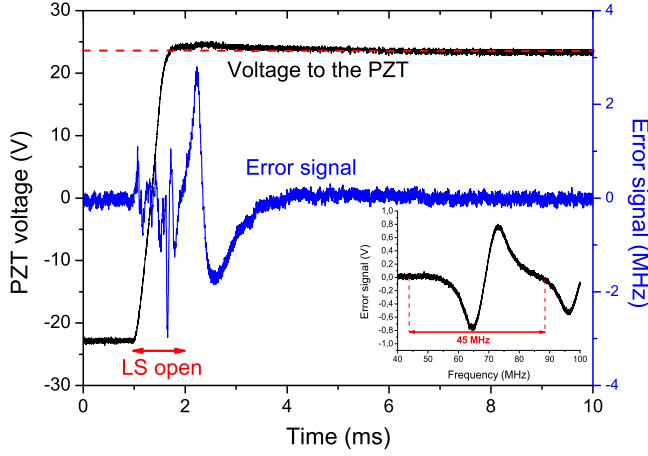


Fig. 3. Behavior of the laser system locked during a frequency step : voltage to the PZT of the EFL (black); error signal (blue). Voltage step of 46.4 V on the PZT, i.e. frequency step of 965.12 MHz on the laser at 780 nm. At the right bottom, error signal with a frequency scan of the laser (@ 780 nm).

waveguide [17] or thanks to free space doubling in a bulk PPLN [4].

In order to determine the frequency noise of the laser, we analyse the noise of the error signal (Fig. 4), which is proportionnal to the frequency of the laser within a bandwidth of 10 kHz (cut-off frequency of the LPF on Fig. 1). We measure first this noise when the laser is unlocked and out of resonance with the atomic transition (in blue). In this configuration we measure only the noise of our electronic lock i.e. the noise on the error signal which does not come from the frequency noise of the laser. When the laser is locked (in green), the noise on the error signal is much lower than the noise of the lock. Thus, the frequency noise of the laser is given by the frequency noise of the lock until a frequency of 3 kHz. We investigate then the origin of the noise on the lock which determines the frequency noise of the laser. The noise on the lock can come mainly from electronic noise, intensity noise of the laser at 50 kHz and etalon effects in the saturated absorption set up which gives a temporal fluctuation of the error signal offset. The origin of the noise can be determined by analyzing the noise on the error signal in different configurations (Fig. 5). In the configuration laser off (in red), one has only the contribution of the electronic noise. In the configuration laser on, out of resonance and PM1 off (in black), one has only the electronic noise and the intensity noise of the laser. In the configuration laser out of resonance, one has the totality of the noise. From the comparison of these configurations, we can deduce that above 1 Hz and below 10 kHz, the noise of the lock comes mainly from the intensity noise of the laser, and below 1 Hz, the noise comes from etalon effects. In conclusion, the frequency noise of our laser below 10 kHz comes from the noise of the lock which is converted into frequency noise in

the feed back loop. The noise of the lock is mainly due to intensity noise of the laser and etalon effects in the saturated absorption set up.

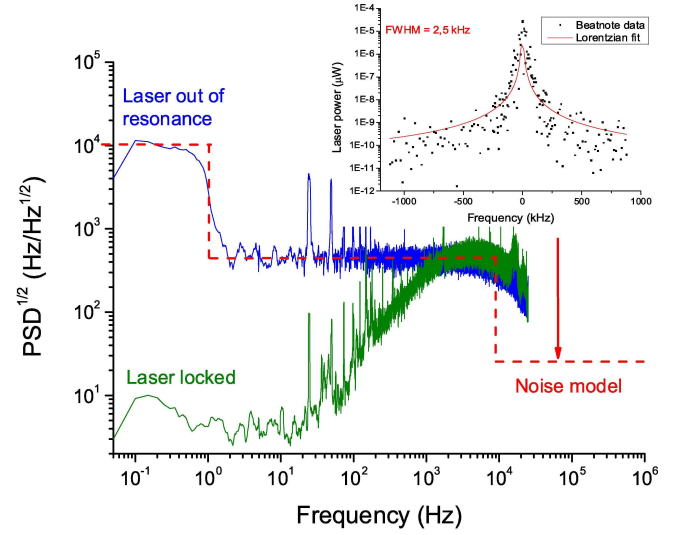


Fig. 4. Square root of the Power Spectral Density (PSD) of the error signal noise : when the laser is locked (green) and when the laser is out of resonance (blue). At the top right, beat note between the EFL and an integrated ECDL with a linewidth lower than 10 kHz. The beat note determines the high frequency part ($f > 10$ kHz) of the frequency noise. The noise of the error signal when the laser is out of resonance (blue) determines the low frequency part ($f < 10$ kHz) of the frequency noise. In red dashes, model used to determine the atom interferometry sensitivity.

In order to estimate the frequency noise of our laser at higher frequency than 10 kHz, we perform a beat note measurement between our locked EFL and an integrated ECDL whose linewidth is specified below 10 kHz (Fig. 4). The lorentzian fit of the wings of the beat note gives us a FWHM linewidth of $\Delta\nu = 2.5$ kHz. Thus, the wings of our laser spectrum behave like a lorentzian curve with a linewidth below 2.5 kHz. These measurements give us informations about frequency noise of the laser at high frequency. Assuming a white noise for the frequency noise of our laser, we can deduce a $\text{PSD}^{1/2}$ of frequency noise below $(S_\nu^0)^{1/2} = (\Delta\nu/\pi)^{1/2} = 28$ Hz/Hz^{1/2} for frequencies above 10 kHz.

We can now estimate the impact of the frequency noise of our laser for acceleration measurements. With the two previous measurements, we can model our laser spectrum by $(S_\nu^0)^{1/2} = 10$ kHz/Hz^{1/2} for $f < 1$ Hz, coming from etalon effects, $(S_\nu^0)^{1/2} = 400$ Hz/Hz^{1/2} for $1 \text{ Hz} < f < 10$ kHz, from intensity noise, and $(S_\nu^0)^{1/2} = 28$ Hz/Hz^{1/2} for $f > 10$ kHz (in red dashes on the Fig. 4). Thus, we can estimate the noise on the atom interferometer measurement induced by the frequency noise of the laser. By using the results of the reference [9] and with classical experimental parameters for a vertical atom accelerometer (the distance atom-mirror for gravimetry, or

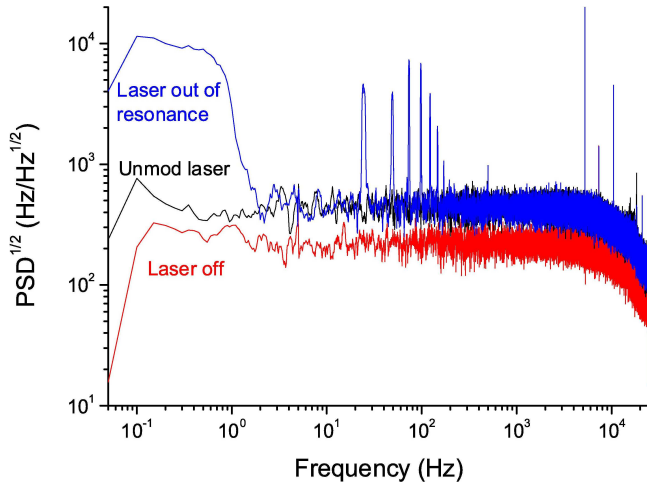


Fig. 5. Square root of the PSD of the error signal noise : when the laser is off (red), when the laser is unmodulated (black) and when the laser is out of resonance (blue).

the distance between the two clouds for gradiometry : $L = 1$ m, the duration of a Raman pulse : $\tau_R = 10 \mu\text{s}$, and the time between two pulses $T = 100$ ms), one obtains a single shot rms noise equal to $\sigma_a = 2,6 \times 10^{-9}$ g, the main contribution coming from low frequency noise between 1 Hz and 10 kHz.

For more demanding applications, this frequency noise could be decreased by improving the saturated absorption set up by subtracting intensity noise of the laser and etalon effect coming from the fiber [18]. The electronic noise could also be decreased by using a higher laser power or a better electronic. With these improvements, it should be possible to obtain a frequency noise of $28 \text{ Hz/Hz}^{1/2}$ on all the frequency range, leading to single shot rms noise equal to $\sigma_a = 6,9 \times 10^{-10}$ g for typical atom accelerometer. In our laser architecture, the EFL could be replaced by an integrated ECDL which is more compact and have comparable laser linewidth. Finally, to get a very compact system, immune to external disturbances, it is possible to realize an all fiber bench with a fibered amplifier and a wave guided PPLN after the PM2 [17].

To conclude, we have developed a tunable narrow linewidth single laser source system for atom interferometry. This system combines the reliability of fiber components and the agility allowed by phase modulators. These features can lead to plug-and-play laser sources for a large number of laboratories developing cold atom experiments. These could be developed for commercial devices, onboard system or fundamental physics space missions. The use of a single laser source significantly reduces failure risks and the amount of additional components for redundancy, particularly critical for space projects. Finally, this architecture could be used for other experiments like the telemetry for the flight formation (satellites) which is an important point for space mission.

We thank F. Nez, from the Laboratoire Kastler Brossel (LKB), for his help on the project. We acknowledge funding support from the Direction Scientifique Générale of the ONERA, the Direction Générale de l'Armement (DGA), and the Centre National d'Etude Spatiale (CNES).

References

1. C. Bordé, *Metrologia* **39**, 435-463 (2002).
2. F. Sorrentino, Kai Bongs, P. Bouyer, L. Cacciapuoti, M. de Angelis, H. Dittus, W. Ertmer, A. Giorgini, J. Hartwig, M. Hauth, S. Herrmann, M. Inguscio, E. Kajari, T. T. Könemann, C. Lämmerzahl, A. Landragin, G. Modugno, F. Pereira dos Santos, A. Peters, M. Prevedelli, E. M. Rasel, W. P. Schleich, M. Schmidt, A. Senger, K. Sengstock, G. Stern, G. M. Tino, and R. Walser, *Microgravity Sci. Technol.* **22**, 551-561 (2010).
3. Y. Bidel, O. Carraz, R. Charrière, M. Cadoret, N. Zahzam, and A. Bresson, *Appl. Phys. Lett.* **102**, 144107 (2013).
4. O. Carraz, F. Lienhart, R. Charrière, M. Cadoret, N. Zahzam, Y. Bidel and A. Bresson, *Appl. Phys. B* **97**, 405-411 (2009).
5. M. Schmidt, M. Prevedelli, A. Giorgini, G.M. Tino, and A. Peters, *Appl. Phys. B* **102**, 11-18 (2011).
6. P. Cheinet, F. Pereira Dos Santos, T. Petelski, J. Le Gouët, J. Kim, K.T. Therkildsen, A. Clairon, and A. Landragin, *Appl. Phys. B* **84**, 643-646 (2006).
7. V. Ménoret, R. Geiger, G. Stern, N. Zahzam, B. Battelier, A. Bresson, A. Landragin, and P. Bouyer, *Dual-wavelength laser source for onboard atom interferometry*, *Opt. Lett.* **36**, 21 (2011).
8. M. Kasevich, and S. Chu, *Phys. Rev. Lett.* **67**, 181 (1991).
9. J. Le Gouët, P. Cheinet, J. Kim, D. Holleville, A. Clairon, A. Landragin, And F. Pereira Dos Santos, *Eur. Phys. J. D*, **44**, 419-425 (2007).
10. A.B. Deb, A. Rakonjac, and N. Kjærgaard, *J. Opt. Soc. Am. B* **29**, 3109 (2012). *Eur. Phys. J. D* **3**, 201-204 (1998).
11. F. Lienhart, S. Boussen, O. Carraz, N. Zahzam, Y. Bidel, and A. Bresson, *Appl. Phys. B* **89**, 177-180 (2007).
12. G. Stern, B. Allard, M. Robert-de-Saint-Vincent, J.-P. Brantut, B. Battelier, T. Bourdel, and P. Bouyer, *Appl. Opt.* **49**, 3092 (2010).
13. W. Liang, V. S. Ilchenko, A. A. Savchenkov, A. B. Matsko, D. Seidel, and L. Maleki, *Opt. Lett.* **35**, 16 (2010).
14. K. Numata, J. Camp, M. A. Krainak, and L. Stolpner, *Opt. Express* **18**, 22 (2010).
15. S. Masuda, A. Seki, and S. Niki, *Appl. Opt.* **46**, 4780 (2007).
16. O. Carraz, R. Charrière, M. Cadoret, N. Zahzam, Y. Bidel and A. Bresson, *Phys. Rev. A* **86**, 033605 (2012).
17. T. Lévêque, L. Antoni-Micollier, B. Faure, and J. Berthon, *Appl. Phys. B* (2013).
18. K. B. MacAdam, A. Steinbach, and C. Wieman, *Am. J. Phys.* **60**, 12 (1992).